Catalysis Today 166 (2011) 194–200

Contents lists available at ScienceDirect

Catalysis Today

journal homepage: www.elsevier.com/locate/cattod

Modified electrode with hydrotalcite-like materials and their response during electrochemical oxidation of blue 69

M.A. Oliver-Tolentino[a], A. Guzmán-Vargas[a,*], A. Manzo-Robledo[b], M.J. Martínez-Ortiz[a], J.L. Flores-Moreno[c]

[a] ESIQIE-IPN, Departamento de Ingeniería Química - Laboratorio de Investigación en Materiales Porosos, Catálisis Ambiental y Química Fina, UPALM Edif.7 P.B. Zacatenco, México, D.F. 07738, Mexico
[b] ESIQIE-IPN, Departamento de Ingeniería Química - Laboratorio de Electroquímica y Corrosión. Edif. Z-5 3er piso, UPALM, Zacatenco, México D.F. 07738, Mexico
[c] Universidad Autónoma Metropolitana-A, Area de Química de Materiales, Avenida San Pablo No. 180, 02200 México D.F., Mexico

ARTICLE INFO

Article history:
Available online 20 September 2010

Keywords:
Hydrotalcite-like materials (LDH)
Oxygen evolution reaction (OER)
Anodic processes
Electro-catalysis
Cation effect

ABSTRACT

In order to evaluate the electrocatalytic properties, Mg/Al and Mg/Ca/Al hydrotalcite-like materials (LDHs) and their corresponding mixed oxide were immersed in a carbon paste electrode matrix to obtain the so-called modified carbon paste electrode (MCPE). Previous to preparation of MCPE, LDH materials were characterized by different techniques, as XRD, FTIR and BET analysis. The electrochemical response of the electrodes was characterized in neutral conditions using reactive blue 69 dye as a probe molecule. Linear sweep voltammetry (LSV), cyclic voltammetry (CV), multi-sweep cyclic voltammetry (MSCV) and open circuit potential transient techniques were employed. Different current magnitudes in the oxygen evolution reaction (OER) were found as a function of thermal treatment and supporting electrolyte (pH). On the other hand, in a solution containing 250 ppm of the probe molecule at neutral pH, peaks attributed to blue 69 oxidation were found at ca. 0.65 and 0.95 V/SCE. The presence of calcium, as additional divalent cation, and the rehydration of the mixed oxide, due to memory effect, have a positive performance, increasing the magnitude of the electrocatalytic process.

© 2010 Elsevier B.V. All rights reserved.

1. Introduction

Layered double hydroxides (LDHs) belong to the anionic clay family or the hydrotalcite-like compounds. These materials have been discovered in Sweden in 1842 [1], but majority of LDHs actually used are obtained by synthesis. LDHs result of the association of divalent and trivalent metallic cations placed in the center of octahedral structures. On the edges, hydroxyl groups are placed. Those octahedral arrangements are joined to form a lamellar structure consisting of brucite-like layers and compensating anions situated in the interlayer space [2]. Hydrotalcite-like compounds can be represented by the general formula:

$$\left[M^{II}_{1-x}M^{III}_{x}(OH)_2\right]^{x+}\left[A^{n-}_{x/n}\right]\cdot mH_2O$$

where x varies from 0.1 to 0.34 [3].

Two of the most important properties of layered double hydroxides are memory effect and anion exchange. In the first one, lamellar structure of LDH is generally stable until 250 °C. Up to this temperature, water physisorbed in the interlayer space is eliminated and the dehydroxilation of the layers and compensation anions decomposition occurs [4]. Since LDH follows a thermal treatment up to 800 °C, periclase (MgO) and spinel ($MgAl_2O_4$) crystalline structures are identified. In the range of 450–600 °C, mixed oxide can be rehydrated to recover the original lamellar structure, as a function of the chemical composition [1]. This property is called "memory effect" and it is usually carried out in vapor phase or in aqueous solution [5]. In the second one, LDH materials present high anionic exchange capacity (2–5 meq/g) [2], which allows their application in different fields. For example, they can substitute anionic exchange resins for the water purification as trap of nitrates, chlorides or phosphates, but also as adsorbents of heavy metals and radioactive elements.

In catalysis, hydrotalcite-like compounds have been tested in several reactions such as epoxydation, aldol and Knoevenagel condensations, halide exchanges, Michael additions, reduction of aldehydes and ketones by hydrogen transfer from alcohols and transesterification reactions, among others [6–8]. After calcination of LDH, mixed oxide are obtained, which are basic solids. Moreover, the preparation of multi-metallic LDHs and their acid–base properties have been widely studied [5,9–11].

Apart from catalysis, LDHs have applications in the very varied domains such as adsorbents, medicaments (anti-acids), additives in the cosmetic and pneumatics industries, PVC stabilizers, corrosion inhibitors and flame retardants [1].

* Corresponding author. Tel.: +52 55 57296000; fax: +52 55 55862728.
E-mail address: aguzmanv@ipn.mx (A. Guzmán-Vargas).

0920-5861/$ – see front matter © 2010 Elsevier B.V. All rights reserved.
doi:10.1016/j.cattod.2010.08.007

Table 1
Chemical composition in wt.%, formula, molar ratio and surface area of the solids.

Sample	Chemical composition (wt.%)					Formula	Molar ratio M^{II}/M^{III}		S_{BET}[a] (m^2/g)
	Mg	Ca	Al	N	C		Solution	Solid	
Mg/Al-HT	21.18	0	7.98	2.12	0.22	$Mg_{0.749}Al_{0.251}(OH)_2(NO_3)_{0.130}(CO_3)_{0.016}$	3	2.98	216
Mg/Ca/Al-HT	16.28	1.07	11.48	2.74	0.54	$Mg_{0.597}Ca_{0.024}Al_{0.379}(OH)_2(NO_3)_{0.174}(CO_3)_{0.040}$	3	1.64	155

[a] The surface areas were determined on the mixed oxide samples.

In this context, mesoporous materials [12], and layered double hydroxides prepared by different synthesis methods, as well as various chemical compositions [13], have been employed in the preparation of modified electrodes. These last materials have been also applied as electrochemical sensors, owing to their anionic exchange capacity to oxidize organic molecules by metallic complexes or surfactants inside the lamellar structure [14,15]. Idemura et al. [16] achieved the reduction of ferrate(III) ions and ligand-exchange during an intercalation process on Mg–Al hydrotalcite-like materials.

Furthermore, it was found that current observed in a clay-modified electrode depends on the porosity, nature, number and activity of the reactive sites [17]. Scavetta et al. [18–20] showed that the electronic conductivity in Ni/Al HDT-like materials can occur due to a complex mechanism involving an "electron hopping" along the layers, which can be attributed to: (i) an inner redox reaction between oxidized and reduced forms of the M^{II}/M^{III} couple and (ii) a migration of anions inside the interlayers to compensate the positive extra-charge. This mechanism depends only on the OH^- desolvation and the adsorption process onto the electrode surface.

In this context, the treatment of wastewater-containing dye compounds is a technological challenge because their catalytic oxidation (treatment more commonly employed) presents some disadvantages. It is well known that the main pollution problem by dyes is their capacity of assimilation–adsorption in water, using ordinary process, causing photosynthesis modification for flora. On the other hand, dye compounds used in textile industry are highly soluble in water, and they show high resistance to the action of chemical agents.

Therefore, an alternative environmental method for the elimination of these pollutants is the so-called advanced oxidation processes (AOPs). AOP is a promising method for the treatment of water contaminated with organic non-biodegradable compounds [21–25].

Azo-dye blue 69 is a synthetic colorant used and wasted by textile industry. This compound shows two main absorbance peaks in the UV–vis region: (i) aromatic ring at 320 nm and (ii) color absorption at 605 nm [26,27]. The main conjugated structures in the blue 69 molecule are the azo group, the benzene and the naphthalene rings; due to the presence of the anion SO_3^- linked to the naphthalene rings, it can be used as a supporting electrolyte. The structure of the molecule is presented in Fig. 1.

In this study, the electrocatalytic response on MCPE with Mg/Al and Mg/Ca/Al hydrotalcite-like materials was evaluated during the electrochemical oxidation of azo-dye blue 69. Electro- and physico-chemical techniques were used to correlate the obtained results.

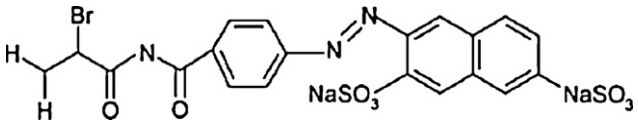

Fig. 1. Chemical structure of dye blue 69.

2. Experimental

2.1. Material preparation

Layered double hydroxides (LDHs), with different M^{II}/M^{III} molar ratios were prepared by coprecipitation method at pH 10 of suitable amounts of $Mg(NO_3)_2{\cdot}6H_2O$, $Al(NO_3)_3{\cdot}6H_2O$ and $Ca(NO_3)_2{\cdot}4H_2O$ (Aldrich, 99.99%, USA) with a 2.0 M solution of NaOH (Aldrich, 99%). The addition of the alkaline solution and pH were controlled by a pH-STAT Tritando apparatus (Metrohm, Switzerland). The suspension was stirred overnight at 80 °C, and then the solid was separated by centrifugation, rinsed thoroughly with distilled water (Na < 100 ppm), and dried overnight at 80 °C. The LDHs were heat-activated in air flow at 450 °C for 4 h (heating rate: 2 °C/min) to yield the $M^{II}(M^{III})O$ mixed oxide. Samples were labeled as Mg/Al-HT, Mg/Ca/Al-HT, for the layered double hydroxides and Mg/Al-Ox and Mg/Ca/Al-Ox, for the corresponding mixed oxide solids.

2.2. Electrode preparation

Modified carbon paste electrodes (MCPEs) were prepared mixing graphite powder (Alfa Aesar, 99.9995%, USA), silicon oil (Aldrich) and the corresponding LDH at 20 wt.%. Then, the mixture was mechanically homogenized and inserted in a 2 mm diameter cylinder (0.0314 cm^2). The surface contact on the MCPE was made with a platinum wire.

2.3. XRD, IR and BET analyses

Chemical analysis of the samples as prepared was performed at the Service Central d'Analyse du CNRS (Solaize, France). XRD patterns of the samples, as prepared or calcined at 450 °C, were recorded on a D8 Focus Bruker AXS instrument using Cu-Kα1 radiation (λ = 1.542 Å, 35 kV, and 25 mA). N_2 sorption experiments at 77 K were carried out on samples previously calcined at 450 °C and outgassed at 280 °C (10 − 4 Pa), with a Micromeritics ASAP 2000 instrument. Specific surface areas were calculated using the BET method. Absorption/transmission IR spectra were run at RT on a Magna-IR Nicolet 750 spectrophotometer, working in the range of wavenumbers 4000–400 cm^{-1} at a resolution of 4 cm^{-1} (number of scans 64).

2.4. Electrochemical measurements

Electrochemical characterization was performed in a conventional three-electrode cell. Carbon rod and saturated calomel electrode (SCE) served as counter and reference electrodes, respectively. Electrochemical techniques, such as cyclic voltammetry (CV), linear sweep voltammetry (LSV), multi-sweep cyclic voltammetry (MSCV) and transient open circuit potential, were employed using a Potentiostat–Galvanostat (Autolab PGSTAT30-2, Switzerland). Distilled water-solution of blue 69 was used as supporting electrolyte and probe molecule. The electrode was immersed into the solution until the open circuit potential (E_{OCP}) was stable. Prior to use, the solution was purged with argon for at least 15 min.

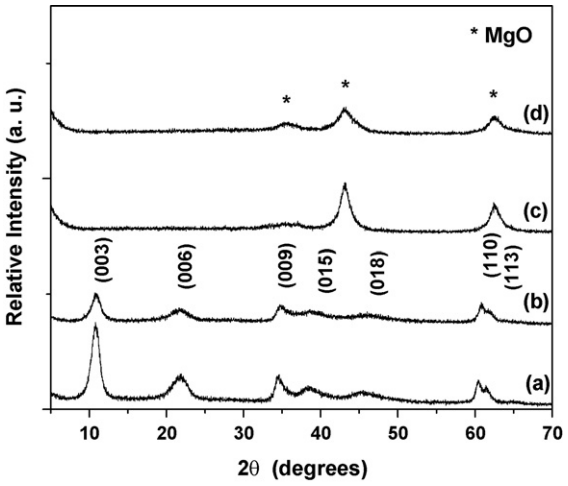

Fig. 2. X-ray diffraction patterns of solids: (a) Mg/Al-HT, (b) Mg/Ca/Al-HT, (c) Mg/Al-Ox, (d) Mg/Ca/Al-Ox.

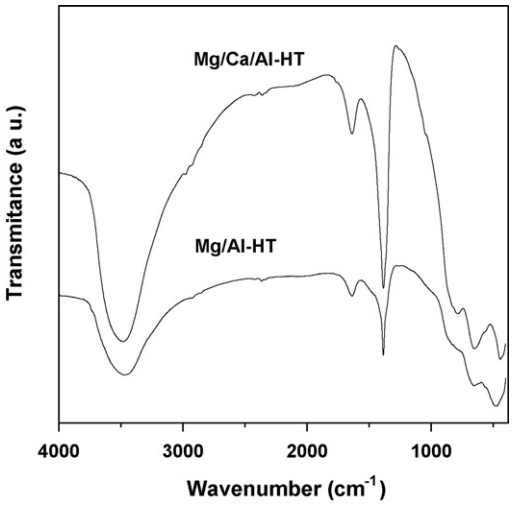

Fig. 3. FTIR spectra of hydrotalcite-like materials.

The potential was scanned toward anodic direction from E_{OCP} to 1.3 V/SCE at scan rate of 20 mV s^{-1}.

3. Results and discussion

3.1. Physico-chemical characterization of LDHs previous to preparation of MCPE

3.1.1. Chemical composition and textural properties

Chemical composition of synthesized hydrotalcite samples and specific surface areas of the calcined solids are reported in Table 1. The M^{II}/M^{III} molar ratio in sample Mg/Al-HT is very similar to that in the nitrate solution used for coprecipitation. Although, molar ratio of sample Mg/Ca/Al-HT was different in the solid to corresponding initial solution, this variation could be attributed to pH synthesis used during the precipitation step. It should be noted that inconsistent results concerning this point are reported in the literature for Ca-containing LDHs [28–30]. On one hand, Grover et al. [28] used a pH of 10 for the LDHs synthesis with different molar ratios; they mention that dissolution could happen due to changes of pH. On the other hand, other authors indicate that only at pH of 11.5 Ca/Al LDH material can be obtained [29,30]. In our case, a low portion of calcium was precipitated, thus, a high quantity still remained in solution. As a consequence, the Al content in the solid resulted higher than expected.

3.1.2. X-ray diffraction

In Fig. 2a and b, all LDH samples showed XRD patterns typical of hydrotalcite-like compounds (JCPDS card 22-0700). The reflections observed are indexed as hexagonal lattices with R3m rhombohedral symmetry, as is usual for LDH's crystalline structure. It should be noted that the (0 0 3) and (0 0 6) lines are broad and the (1 1 0) and (1 1 3) lines are well defined in two LDH samples. For the calcined solids (c and d), they present characteristic peaks corresponding to the periclase phase of MgO (JCPDS file 04-0829), Mg/Al and Mg/Ca/Al mixed oxide are formed, resulting from the collapse of the layered structure.

3.1.3. Infrared spectroscopy

The FTIR spectra in the 4000–400 cm^{-1} region of the as-synthesized Mg/Al-HT and Mg/Ca/Al-HT are shown in Fig. 3. For Mg/Al-HT, the wide band at 3465 cm^{-1} is assigned to the hydrogen-bonding stretching vibrations of OH^- groups. This band can be mainly attributed to the Al–OH bond, but it can be perturbed by nearby Mg cations [31]. In the case of Mg/Ca/Al, this band is observed at 3480 cm^{-1}. This shift can be due to the presence of Ca ions in the brucite-like sheets. At lower wavenumbers, Mg/Al-HT exhibits two main bands located at 1637 and 1384 cm^{-1}. The first band is due to the ν-OH bending from water trapped in the interlayer region, whereas 1384 cm^{-1} band is assigned to the nitrate $\nu 3$ antisymmetric stretching modes. No appreciable changes were noted in the band positions of Mg/Ca/Al-HT, since these bands are observed at 1637 and 1382 cm^{-1}. Finally, the region <1000 cm^{-1} gives information about lattice vibrations and M–OH stretching and M–OH–M′ bending vibrations. Bands situated in this region are sensible to compositional variations as observed for the 478 and 443 cm^{-1} bands shown by Mg/Al-HT and Mg/Ca/Al-HT, respectively.

3.2. Linear and cyclic voltammetry characteristics

Fig. 4 shows the *i–E* characteristics obtained during the positive–negative going scan in a solution containing 250 ppm of azo-dye blue 69 at scan rate of 20 mV/s for LDH samples (Fig. 4A), and calcined samples (Fig. 4B, corresponding to $M^{II}(M^{III})O$ mixed oxide). In this figure, profiles (a) represent the unmodified carbon paste electrode (UCPE), whereas profiles (b) correspond to the modified carbon paste electrode (MCPE) with Mg/Al-HT and Mg/Al-Ox, and (c) to Mg/Ca/Al-HT and Mg/Ca/Al-Ox.

These characteristics exhibit two anodic peaks at ca. 0.65 and 0.95 V/SCE and a cathodic peak at 0.55 V/SCE. The anodic processes could be associated to oxidation in two different positions (i.e. at the azo or aryl group) [26,27,32]. The low current magnitude in the negative-going scan, corresponding to a reversible process, should be due to the stability of the products formed at the interface during oxidation.

The intensity of these anodic processes depends on the MCPE nature and heat treatment. According to this, Mg/Ca/Al (profile c) showed the major activity during the positive going scan. Moreover, the current magnitude is more intense for the mixed oxide samples (Fig. 4B-c). Therefore, for these samples in contact with colorant aqueous solution, the LDH structure is recovered (memory effect) trapping OH^- ions from water. At these conditions, colorant must be adsorbed in the interlayer space due to the presence of $-SO_3^-$ species, generating and increasing current intensities associated to oxidation reactions. Conversely, in HT samples, the adsorption of colorant presents more kinetic-diffusion difficulties due to the presence of NO_3^- ions, making the oxidation process less intense. This fact could be associated to low anion exchange ratio between

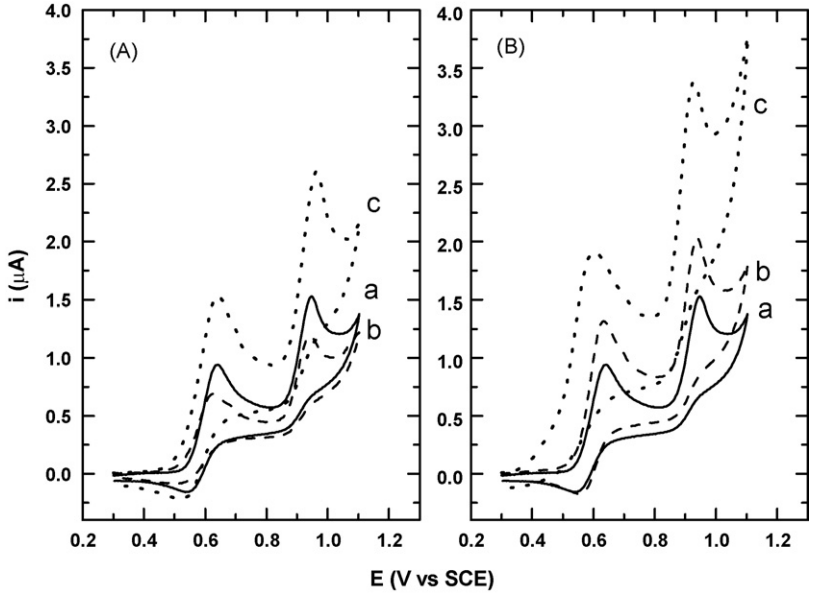

Fig. 4. Cyclic voltammograms of blue 69 (250 ppm) (a) UCPE, (b) Mg/Al, (c) Mg/Ca/Al, (A) HT, (B) mixed oxide.

NO_3^- and SO_3^- at the electrode surface. It is also well known that activation step in LHD materials by calcination and rehydration increases anion exchange capacity as well as basic properties [5]. In this case, it should also be noted in Table 1 that Mg/Ca/Al has an anion exchange capacity greater than Mg/Al sample in agreement with electrochemical process described above.

In order to observe a possible effect of the supporting electrolyte on the oxidation process described previously, similar experiments were carried out with Mg/Ca/Al modified electrodes in 250 ppm blue 69 + NaCl 0.1 M as electrolyte. The results are shown in Fig. 5 (Fig. 5A for HT and Fig. 5B for the corresponding mixed oxide samples). In this figure, only the positive going scan is shown for simplicity. As it is observed, the profiles exhibit similar characteristics than those obtained in Fig. 4. However, the current intensity in absence (profile a), is higher than in solution-containing NaCl (profile b). This behavior could be associated to the nature and preference of exchange anions at the interlayer space, which is in the order $OH^- > F^- > Cl^- > Br^- > NO_3^- > I^-$ [2]. Therefore, the adsorption in the interlayer space is dominated by Cl^- ions instead of blue 69 molecule. Based on these results, it can be suggested that the evolution of electrochemical processes in blue 69-based solutions is associated to: (i) nature of the UCPE, (ii) heat treatment and (iii) supporting electrolyte.

In order to verify the results already discussed, experiments in solutions free of colorant were performed. Fig. 6 presents the *i*–*E* characteristics for MCPE in NaCl 0.1 mol/L as supporting electrolyte for UCPE (profile a), Mg/Ca/Al-HT (profile b) and Mg/Ca/Al-Ox (profile c) samples. It is interesting to observe that no peaks associated to probe molecule interaction are evidenced, as expected. The profiles found in these characteristics are assigned to the oxygen evolution reaction (OER) promoted by the OH^- ion concentration and the nature (pH) of the supporting electrolyte as well as the electrode in turn. Thus, at these conditions, Mg/Ca/Al-Ox electrode presents higher catalytic activity toward OER than Mg/Ca/Al-HT

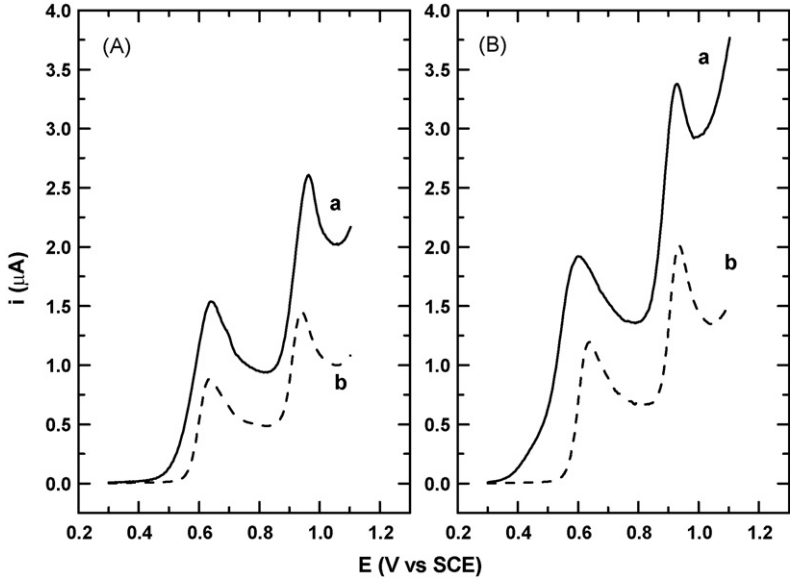

Fig. 5. Linear voltammograms of blue 69 (250 ppm) (a) free of NaCl, (b) with 0.1 M NaCl, (A) Mg/Ca/Al-HT, (B) Mg/Ca/Al-Ox.

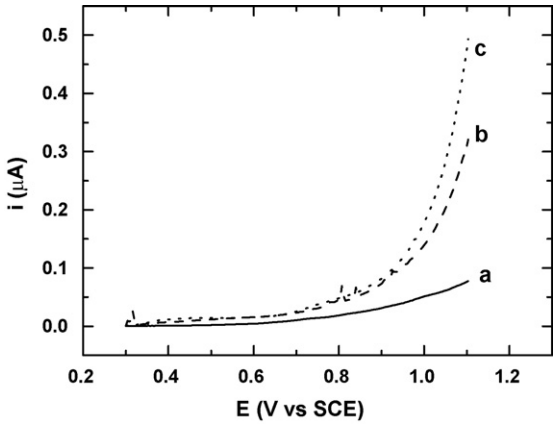

Fig. 6. Linear sweep voltammograms in 0.1 M NaCl, (a) UCPE, (b) MCPE Mg/Ca/Al-HT, (c) MCPE Mg/Ca/Al-Ox.

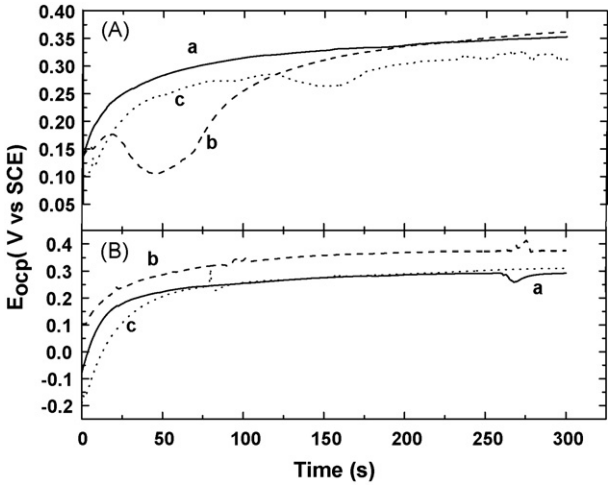

Fig. 7. OCP evolution versus the immersion time of MCPE, (A) Mg/Ca/Al-HT, (B) Mg/Ca/Al-Ox, (a) in 0.1 M NaCl, (b) 250 ppm of blue 69 + 0.1 M NaCl, (c) 250 ppm of blue 69.

sample, associated to the ionic charge transfer mechanism, which depends only on the OH^- desolvation, and adsorption processes onto the electrode–electrolyte interface [18–20], the UCPE showed lower activity, as predictable.

3.3. Open circuit potential as a measure of surface state

The open circuit potential (E_{OCP}) is a measurement without a net current flow through the external circuit of electrochemical systems. It has been established as a sensitive and effective measure for monitoring spontaneous phenomena at zero current occurring in the electrode–electrolyte interface such as in metal corrosion [33], for monitoring of cation exchange in electrodes modified with zeolite [34] and for interfacial interactions of ionic species and gases [34–36]. Therefore, temporal transients of open circuit potential (E_{OCP}-t) applied to the MCPE–solution interface could be a sensitive resource for a major understanding on the behavior of electrochemical phenomena with regard to anionic exchange dynamics. For such an approach, the OCP evolution for HT and mixed oxide modified electrodes was monitored (Fig. 7). These measurements were compared among NaCl (profile a), NaCl + blue 69 (profile b) and blue 69 (profile c) solutions. The initial OCP in Mg/Ca/Al-Ox electrode (Fig. 7B) is more negative than HT sample, and the OCP changes with the immersion time, until reaching a maximum. This phenomenon is associated to the adsorption of anions during the recovery structure (memory effect) of the LDH structure; while that for HT sample, an ionic exchange occurs spontaneously between anions of the supporting electrolyte nature: Cl^-/OH^- (profile a), Cl^-/OH^-/blue 69-SO_3^- (profile b) and OH^-/blue 69-SO_3^- (profile c) and the NO_3^- ions compensate the charge in HT sample; until reaching thermodynamic potential.

3.4. Multi-sweep cyclic voltammetry (MSCV)

Fig. 8 shows the multi-sweep cyclic voltammetry profiles for azo-dye based solution (400 ppm) at neutral pH for MCPE with Mg/Ca/Al-HT (Fig. 8A) and Mg/Ca/Al-Ox (Fig. 8B). Notice that these profiles are similar to those found by cyclic voltammetry (see Fig. 4). The current magnitude in these characteristics decreases considerably after the first cycle, indicating a strong adsorption of blue 69 on MCPE [37]. However, the current ratio is higher in the calcined

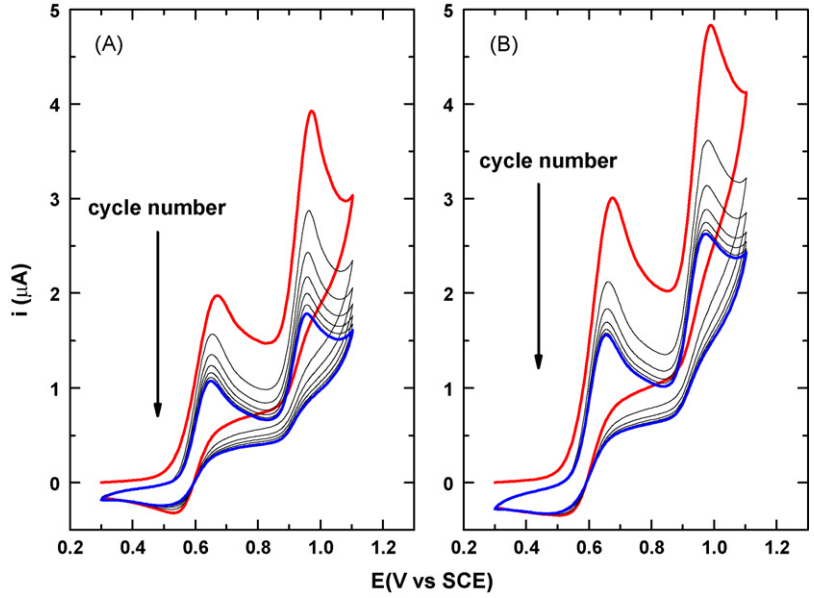

Fig. 8. Multi-sweep cyclic voltammograms of blue 69 (400 ppm), electrode modified with (A) Mg/Ca/Al-HT, (B) Mg/Ca/Al-Ox. First scan is the red line and the last scan is the blue line. (For interpretation of the references to color in this figure legend, the reader is referred to the web version of the article.)

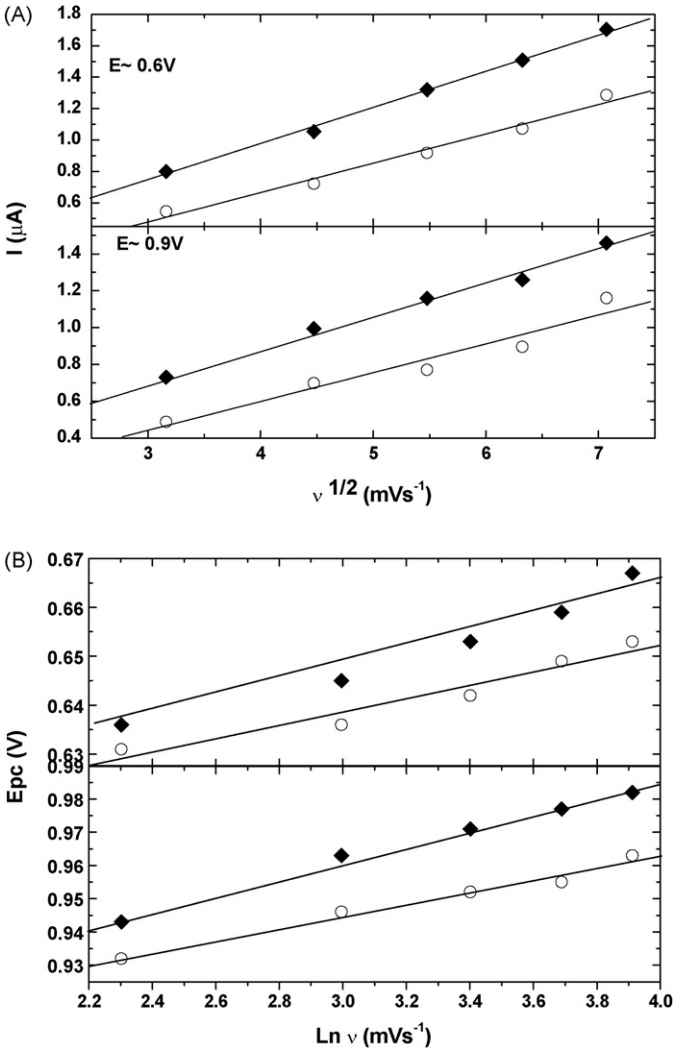

Fig. 9. (A) Peak current as a function of the scan rate in solution of blue 69 (400 ppm). (B) Relationship between anodic peak potential (E_{pa}) and ln ν. Electrode modified with (◯) Mg/Ca/Al-HT and (♦) Mg/Ca/Al-Ox.

sample (Mg/Ca/Al-Ox). Under these conditions, the probe molecule interacts with the electrode interface in the first cycle. During the interval of the immersion time, large quantities of azo-dye are oxidized, becoming electrochemically accessible for charge transfer redox reactions.

3.5. Effect of scan rate and blue 69 concentration

3.5.1. Scan rate

The analysis of the blue 69 faradic current as a function of scan rate for the MCPE with Mg/Ca/Al-HT is presented in Fig. 9A. The results obtained in these characteristics reveal a linear relationship (I_p versus $\nu^{1/2}$) for both main oxidation peaks. This behavior indicates that the oxidation of blue 69 on MCPE is an adsorption-controlled process, as discussed in Section 3.4. Moreover, it can be established that the electrode process is highly irreversible (see Section 3.2). Taking into account these assumptions, Laviron's equation (1) [38] can be used to calculate some electrochemical parameters related to the redox process, as usually employed for electrochemical studies [37,39].

$$E_{pa} = E^0 + \frac{RT}{\alpha nF} \ln \frac{RTk_s}{\alpha nF} + \frac{RT}{\alpha nF} \ln \nu \quad (1)$$

Table 2
Parameters of Eq. (1) obtained from Fig. 9 and reaction order (m) calculated from Fig. 10.

	MCPE	
	Mg/Ca/Al-HT	Mg/Ca/Al-Ox
E = 0.6 V		
k_s (seg^{-1})	11.49	13.88
αn	1.38	1.86
m	1.0915	1.072
E = 0.9 V		
k_s (seg^{-1})	7.58	8.42
αn	1.18	1.42
m	1.1	1.056

where E_{pa} is the potential of anodic peak, α is the transfer coefficient, k_s is the standard rate constant in the vicinity of the electrode surface, n is the number of electrons transferred, ν is scan rate, E^0 is the formal potential, T = 298 K, R = 8.314 J/mol K and F = 96,480 C/mol. In this equation, E^0 is obtained from data given in an E_{pa} versus ν plot at ν = 0 (figure not shown); the corresponding E^0 values obtained were 0.62 and 0.93 V for the two main anodic processes observed in Fig. 4. On the other hand, according to Eq. (1) αn and k_s can be calculated from data in Fig. 9B.

Table 2 summarizes the parameters obtained from Fig. 9, it can be observed that αn and k_s values are higher for Mg/Ca/Al-Ox electrodes, the results are associated to the major electrocatalytic activity in mixed oxide samples.

3.5.2. Blue 69 concentration

With the purpose to determine the reaction order, experiments with different initial concentrations of reactant (50–400 ppm) were carried out. The reaction order can be determined from the slope (m) of straight lines obtained of log(i) versus log(blue 69) illustrated in Fig. 10 [40]. Consequently, and using this information, the reaction order calculated is approximately 1 (Table 2). In addition, the profiles show that the anodic current behavior is linked to dye-molecule concentration.

3.6. Temperature effect

As in the case of concentration, studies as a function of temperature were carried out in the modified electrodes. The results are reported (Fig. 11) in terms of charge (Q, μC) for Mg/Ca/Al-HT (◯) and Mg/Ca/Al-Ox (♦) samples at two different potentials corre-

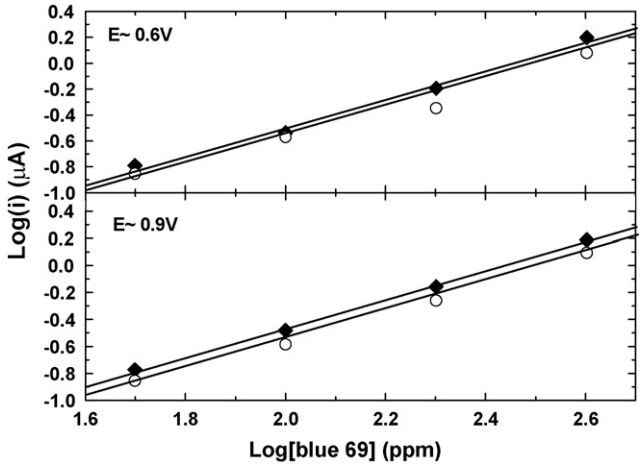

Fig. 10. Current versus blue 69 concentration (C) profile, electrode modified with (◯) Mg/Ca/Al-HT, (♦) Mg/Ca/Al-Ox.

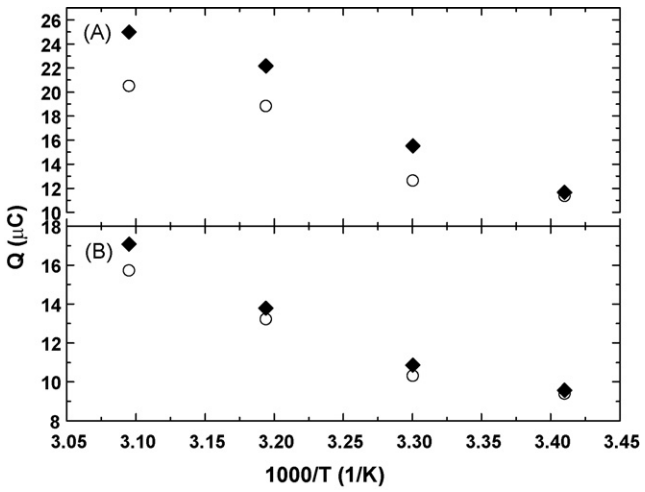

Fig. 11. Charge (Q) versus temperature (T), Q was calculated from 0.5 to 0.8 V (A) and 0.8 to 1.1 V (B). Electrode modified with (○) Mg/Ca/Al-HT, (♦) Mg/Ca/Al-Ox.

sponding to the two main oxidation peaks. It should be mentioned that the charge was associated to the area under the curve from the graph current versus time (not shown). In these experiments, the charge was calculated between 0.5–0.8 and 0.8–1.1 V. According to these profiles, the catalytic behavior of the hydrotalcites promotes an important enhancement versus dye oxidation as temperature increases.

Therefore, the electrochemical processes at the vicinity of the electrode surface and the diffusion of reactive species toward it are improved by the dye-concentration and temperature conditions, increasing the adsorption capacity onto the hydrotalcite-layer mixed in the carbon-support matrix.

4. Conclusions

LDH like materials, dried and calcined, mixed in a carbon matrix were evaluated in blue 69 azo-dye oxidation, they showed a catalytic effect in the electrochemical process due to their adsorption capacity. No significant changes were observed by FTIR spectroscopy on typical band assignment between Mg/Al-HT and Mg/Ca/Al-HT samples, in agreement with those reported by XRD.

The presence of calcium in LDH structure (Mg/Ca/Al) promotes better catalytic performance than its counterpart Mg/Al caused by an increase of the adsorption capacity due to M^{II}/M^{III} molar ratio, as demonstrated by electrochemical techniques. In addition, the heat treatment enhances such as performance due to LDH-structural modification obtaining the mixed oxide structure that, after rehydration, samples recover the hydrotalcite phase by memory effect property. Finally, studies as a function of solution temperature and dye-concentration indicated that the kinetic-diffusion processes can be improved, increasing the adsorption capacity onto the LDH-interlayer space and in the carbon-support matrix.

Acknowledgments

Projects: SIP-IPN 20090258, 20090868, 20090921; CONACYT 61079, 61597; and ICyTDF-PICS08-29 for financial support.

References

[1] F. Cavani, F. Trifirò, A. Vaccari, Catal. Today 11 (1991) 173–301.
[2] S. Miyata, Clays Clay Miner. 31 (1983) 305–311.
[3] S. Miyata, Clays Clay Miner. 28 (1980) 50–56.
[4] W.T. Reichle, J. Catal. 94 (1985) 547–557.
[5] J. Sanchez-Valente, F. Figueras, M. Gravelle, P. Kumbhar, J. Lopez, J.P. Besse, J. Catal. 189 (2000) 370–381.
[6] D. Tichit, B. Coq, Cattech 7 (2003) 206–217.
[7] M.J. Martínez-Ortiz, D. Tichit, P. Gonzalez, B. Coq, J. Mol. Catal. A 201 (2003) 199–210.
[8] B.M. Choudary, M. Lakshmi-Kantam, C. Venkat-Reddy, S. Aranganathan, P. Lakshmi-Santhi, F. Figueras, J. Mol. Catal. A 159 (2000) 411–416.
[9] F. Prinetto, M. Manzoli, G. Ghiotti, M.J. Martínez-Ortiz, D. Tichit, B. Coq, J. Catal. 222 (2004) 238–249.
[10] D. Tichit, A. Rolland, F. Prinetto, G. Fetter, M.J. Martínez-Ortiz, M.A. Valenzuela, P. Bosch, J. Mater. Chem. 12 (2002) 3832–3838.
[11] V.R.L. Constantino, T.J. Pinnavaia, Inorg. Chem. 34 (1995) 883–892.
[12] D. Fattakhova-Rohlfing, J. Rathouský, Y. Rohlfing, O. Bartels, M. Wark, Langmuir 21 (2005) 11320–11329.
[13] R. Roto, G. Villemure, Electrochim. Acta 51 (2006) 2539–2546.
[14] L. Fernández, H. Carrero, Electrochim. Acta 50 (2005) 1233–1240.
[15] M. Li, S. Chen, F. Ni, Y. Wang, L. Wang, Electrochim. Acta 53 (2008) 7255–7260.
[16] S. Idemura, E. Suzuki, Y. Ono, Clays Clay Miner. 37 (1989) 553–557.
[17] A. Fitch, Clays Clay Miner. 38 (1990) 391–400.
[18] E. Scavetta, D. Tonelli, M. Giorgetti, F. Nobili, R. Marassi, M. Berrettoni, Electrochim. Acta 48 (2003) 1347–1355.
[19] E. Scavetta, M. Berrettoni, F. Nobili, D. Tonelli, Electrochim. Acta 50 (2005) 3305–3311.
[20] E. Scavetta, B. Ballarin, M. Berrettoni, I. Carpani, M. Giorgetti, D. Tonelli, Electrochim. Acta 51 (2006) 2129–2134.
[21] R. Bauer, G. Waldner, H. Fallmann, S. Hager, M. Klare, T. Krutzler, S. Malato, P. Maletzky, Catal. Today 53 (1999) 131–144.
[22] Z.D. Wei, M.B. Ji, S.G. Chen, Y. Liu, C.X. Sun, G.Z. Yin, P.K. Shen, S.H. Chan, Electrochim. Acta 52 (2007) 3323–3329.
[23] M.S. El-Deab, M.E. El-Shakre, B.E. El-Anadouli, B.G. Ateya, Int. J. Hydrogen Energy 21 (1996) 273–280.
[24] M.S. El-Deab, M.I. Awad, A.M. Mohammad, T. Ohsaka, Electrochem. Commun. 9 (2007) 2082–2087.
[25] C.G. Joseph, G. Li-Puma, A. Bono, D. Krishnaiah, Ultrason. Sonochem. 16 (2009) 583–589.
[26] G. Zacahua-Tlacuatl, J.J. Castro-Arellano, A. Manzo-Robledo, Chem. Eng. Commun. 196 (2009) 1178–1188.
[27] S.L. Orozco, E.R. Bandala, C.A. Arancibia-Bulnes, B. Serrano, R. Suárez-Parra, I. Hernández-Pérez, J. Photochem. Photobiol. A 198 (2008) 144–149.
[28] K. Grover, S. Komarneni, H. Katsuki, Water Res. 43 (2009) 3884–3890.
[29] L. Vieille, E.M. Moujahid, C. Taviot-Guého, J. Cellier, J.P. Besse, F. Leroux, J. Phys. Chem. Solids 65 (2004) 385–393.
[30] R. Segni, L. Vieille, F. Leroux, C. Taviot-Guého, J. Phys. Chem. Solids 67 (2006) 1037–1042.
[31] J.T. Kloprogge, R.L. Frost, J. Solid State Chem. 146 (1999) 506–515.
[32] E.M. Ungureanu, A.C. Razus, L. Birzan, M.S. Cretu, G.O. Buica, Electrochim. Acta 53 (2008) 7089–7099.
[33] S.A. Salih, A.N. Elmasri, A.M. Baraka, J. Mater. Sci. 36 (2001) 2547.
[34] A.M. Melendez, E. Lima, I. González, J. Phys. Chem. C 112 (2008) 17206–17213.
[35] R.A. Manzhos, Y.M. Maksimov, B.I. Podlovechenko, Russ. J. Electrochem. 41 (2005) 832.
[36] B.I. Podlovchenko, T.D. Gladysheva, E.A. Kolyadko, J. Electroanal. Chem. 552 (2003) 85.
[37] W. Sun, K. Jiao, X. Wang, L. Lu, J. Electroanal. Chem. 578 (2005) 37–43.
[38] E. Laviron, J. Electroanal. Chem. 101 (1979) 19–28.
[39] H. Yin, L. Cui, S. Ai, H. Fan, L. Zhu, Electrochim. Acta 55 (2010) 603–610.
[40] R.N. Singh, T. Sharma, A. Singh, Anindita, D. Mishra, S.K. Tiwari, Electrochim. Acta 53 (2008) 2322–2330.